



2019

# RESEARCH JOURNAL

UNDERGRADUATE  
RESEARCH  
PROGRAM

**UCLA** Samueli  
School of Engineering

## Table of Contents

### Student Research Abstracts & Posters

2	Brian Chap	16	Manu Saravanan
4	Jessica Chun	18	Alexander Soohoo
6	Ashley Dickman	20	Alison Tran
8	Adrien Hadj-Chaib	22	Peter Wang
10	Omar Issa	24	William Whitehead
12	Alexis Joo		
14	Kayli Masuda		

### Poster Symposium and Awards Ceremony | May 21, 2019

5:00 PM - 5:05 PM	Announcement (William Herrera)
5:05 PM - 5:50 PM	Poster presentations – DCAB will use a 10-point rubric to score each poster
5:50 PM - 6:00 PM	Break / Transition to Mong Auditorium for Awards Ceremony
6:00 PM - 6:30 PM	Awards Ceremony – Dean Murthy will be giving a short welcome and discuss the importance of undergraduate research. Dean Murthy will then be handing out certificates and awards.



## DEAN'S MESSAGE

The Undergraduate Research Program's (URP) provides participants with research experience in a wide range of engineering fields. Undergraduate students participate in research with UCLA faculty and research teams to gain real-world lab experience. URP's mission is to help students communicate the results of their research projects. As part of this program, URP students:

- Meet and network with peers who have similar goals and interests
- Learn to communicate research outcomes by participating in Technical Presentation Labs
- Create a professional scientific poster of their research
- Write and publish a research abstract
- Present a detailed Summary of Project
- Become more competitive when applying to engineering graduate schools

This year, 12 Samueli undergraduate students were selected to join the 2018-19 URP cohort. I would like to congratulate this 2nd URP class on completing their amazing research projects. Creating new knowledge is a very important, and very difficult, task. These high-performing students have done an outstanding job balancing their normal academic course load with the rigorous demands of research. They should be very proud of the abstracts and posters they have published today. I encourage you to meet the students, ask questions about their projects, and learn about the amazing new knowledge that is being created here at the UCLA Samueli School of Engineering.

Sincerely,

Jayathi Murthy  
Ronald and Valerie Sugar Dean



Brian Chap  
Electrical Engineering  
Freshman

LAB NAME

Device Research Lab

FACULTY ADVISOR

Kang L. Wang & Philippe Sautet

GRADUATE STUDENT DAILY LAB SUPERVISOR

N/A

DEPARTMENT

Electrical and Computer Engineering

# First-Principles Study of the Proximity Effect Between a Topological Insulator and an Antiferromagnet

Proximity effects between topological insulators (TIs) and magnetic materials are currently one of the most promising approaches to realizing the room-temperature Quantum Anomalous Hall Effect (QAHE), with potential applications in dissipationless transistors, magnetic sensing, and motion sensing. First-principles calculations using the Vienna ab initio simulation package (VASP) for density-functional theory (DFT) are performed on the interfaces between Bi<sub>2</sub>Se<sub>3</sub> and Bi<sub>2</sub>Te<sub>3</sub> TI and the antiferromagnet CrSb, selected for its similar lattice parameters that enable accurate measurement and high Ne 'el temperature. Results are also pending for the ferrimagnet BaM (BaFe<sub>12</sub>O<sub>19</sub>), chosen for its insulating behavior, via the Perdew-Burke-Ernzerhof (PBE) functional. The first-principles study is expected to be the first to analyze the proximity effect between a TI and a ferrimagnet, with the effects of vary- ing quintuple layers and Se/Te substitutions in the heterostructure incorporated. Analysis of the charge contributions of atoms in the heterostructure and spin-DOS calculations are performed and experimental verification of the BaM data is expected to occur in the near future. Combined with the relative affordability of most materials used in this study, the case for using the proximity effect in order to establish QAHE at room temperature is anticipated to be greatly strengthened, with foreseeable uses in quantum computing and non-volatile, high speed, and high density memory resistant to damage.

## First-principles study of the proximity effect between a topological insulator and an antiferromagnet

Brian Chap, Prof. Kang L. Wang, Prof. Philippe Sautet



### The Big Picture

Topological insulators (TI): insulating interior, conducting exterior  
A wide array of applications: spintronics, dissipationless transistors, quantum computing, holograms, magnetic and motion sensing, non-volatile, high-speed, dense memory resistant to physical alteration

Quantum Hall Effect (QHE): quantized Hall conductance (good for data)  
Anomalous Hall Effect (AHE): ferromagnet (FM) "enhancement"  
Quantum Anomalous Hall Effect (QAHE): no external magnetic field  
TIs display QAHE at their 2-D surface states

QAHE currently occurs at low temperatures (< ~100 K)  
The proximity effect is favored over doping instability

To what extent can a better theoretical understanding of the Bi<sub>2</sub>Se<sub>3</sub>/CrSb/Bi<sub>2</sub>Te<sub>3</sub>/CrSb systems help realize room-temperature QAHE?

### Materials

Bi<sub>2</sub>Se<sub>3</sub>: simple band structure, large band gap (~0.3 eV), potentially inexpensive fabrication  
CrSb: high Ne'el temperature (~700 K), lattice matching, RT magnetization of Cr (~3 μB)  
Antiferromagnets (AFMs): external field resistance, work frequencies (~10 to 1000 GHz)  
6x6x1 1-QL heterostructures, 8x8x1 2-QL heterostructures  
Quintuple layer (QL): 5 atoms (Bi-Se/Te-Bi-Se/Te-Bi)

Figure 2: Projected density of states: For the closest Cr atom to the TI in the Bi<sub>2</sub>Se<sub>3</sub> heterostructure with 2 QLs, relative to the Fermi level.

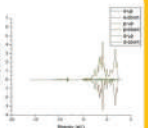
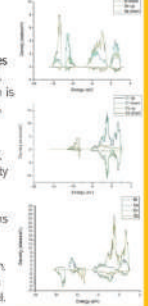


Figure 5: Density of states = calculated. As expected, the largest magnetization is recorded in the Cr atoms, while the magnetization distributions of Bi and Se/Te are heavily aligned, implying that the proximity effect impacts both elements similarly. For positive spin, the Bi atoms peak at higher energies than Se or Te, indicating lower electron occupation. Energies are plotted with respect to the Fermi level.



### Methods

First-principle calculations are conducted using the Vienna ab-initio software package (VASP)  
- Wide usage in the scientific community  
- Expansive set of pseudopotentials  
- Efficiency

Convergence threshold: 1 x 10<sup>-6</sup> eV/Å  
Spin-orbit coupling after geometric optimization

Additional software: p4vasp, OriginLab, Materials Studio, VESTA, Hoffman2 supercluster

Projected density of states (PDOS) to determine origins of magnetization

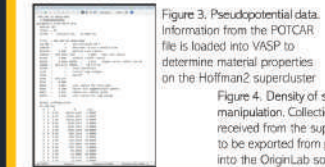


Figure 3: Pseudopotential data. Information from the POTCAR file is loaded into VASP to determine material properties on the Hoffman2 supercluster



Figure 4: Density of states manipulation. Collection of data received from the supercluster, to be exported from p4vasp into the OriginLab software

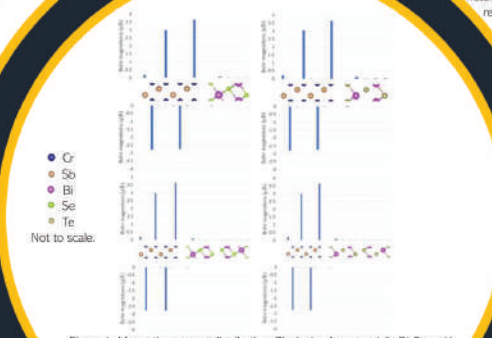


Figure 1: Magnetic moment distribution. Clockwise from top left: Bi<sub>2</sub>Se<sub>3</sub> with 1 QL, Bi<sub>2</sub>Te<sub>3</sub> with 1 QL, Bi<sub>2</sub>Te<sub>3</sub> with 2 QLs, and Bi<sub>2</sub>Se<sub>3</sub> with 2 QLs. From the distribution, it could be clearly understood that the proximity effect exists between the CrSb substrate and Bi<sub>2</sub>Se<sub>3</sub>/Bi<sub>2</sub>Te<sub>3</sub> TI. The characteristic antiferromagnetic spin distribution of CrSb is mimicked in the TI material, and the values obtained are realistic when compared to similar heterostructures.

### The Case for BaM

BaFe<sub>12</sub>O<sub>19</sub> (BaM): relatively inexpensive ferrimagnet  
More easily detectable than AFMs, while also maintaining AFM benefits  
BaM: High Curie temperature (~723 K), resistant to corrosion and chemicals  
Unique first-principles study of the proximity effect between a TI and a ferrimagnet



Figure 6: Cross-sectional TEM of BaM interface. Schematic of BaM's structure with respect to the quintuple layers of Bi<sub>2</sub>Se<sub>3</sub>.  
\*Yang, W., et al. (2014)

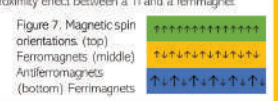


Figure 7: Magnetic spin orientations. (top) Ferromagnets (middle) Antiferromagnets (bottom) Ferrimagnets

### References

Ando, L., et al. Layered and non-layered magnetotransport in heterostructures. Nat. Phys. 11, 1014-1018 (2015).  
Bianchi, F., et al. Superconductivity in three-dimensional (3D) d-wave superconductors. Phys. Rev. B 83, 020501 (2011).  
Buehler, R., et al. Measurement of topological quantum computation via double-heterostructure. Phys. Rev. B 87, 051413 (2013).  
Chang, C.-Z., et al. Quantum anomalous Hall effect in three-dimensional layered topological insulators. Nat. Phys. 8, 1361-1365 (2012).  
Chang, C.-Z. A Quantum Study on Topological Properties of Surface States. Ph.D. Thesis, Princeton University, 2014.  
Fu, L., et al. Topological surface states and their spin and orbital magnetic moments. Phys. Rev. Lett. 108, 236803 (2012).  
Götz, D., et al. Quantum anomalous Hall effect in a topological insulator. Nat. Phys. 8, 1361-1365 (2012).  
He, S.-L., et al. Magnetic ordering in a topological insulator. Nat. Phys. 8, 1361-1365 (2012).  
Hofstadter, D., et al. Topological quantum anomalous Hall effect in a topological insulator. Nat. Phys. 8, 1361-1365 (2012).  
Huang, S.-Y., et al. Proximity effect induced topological phase transition in a topological insulator. Nat. Phys. 8, 1361-1365 (2012).  
Jain, J. C., et al. The quantum anomalous Hall effect: theory and experiment. arXiv:1408.0208 (2014).  
Miyah, M., et al. Spin-orbit torque generated by a topological insulator. Nat. Phys. 8, 1361-1365 (2012).  
Oshrokh, M. M., et al. Breaking time-reversal symmetry of the topological insulator surface by metal organic coordination networks. Phys. Rev. B 86, 160309 (2012).  
Wang, L., et al. Quantum anomalous Hall effect in a topological insulator. Nat. Phys. 8, 1361-1365 (2012).  
Yang, W., et al. Proximity effect between a topological insulator and a magnetic insulator with large perpendicular anisotropy. Appl. Phys. Lett. 103, 022101 (2013).  
Zhang, S. Z., et al. Magnetic and electronic properties of a topological insulator. Nat. Phys. 8, 1361-1365 (2012).  
Zhang, S. Z., et al. Superconductivity in a topological insulator. Nat. Phys. 8, 1361-1365 (2012).

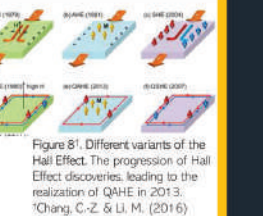


Figure 8: Different variants of the Hall Effect. The progression of Hall Effect discoveries, leading to the realization of QAHE in 2013.  
\*Chang, C.-Z. & Li, M. (2016)

### Acknowledgements

In addition to Prof. Kang L. Wang and Prof. Philippe Sautet, I would also like to thank Prof. Georg Kresse, University of Vienna, Austria; Gen Yin, Haiyang Wang, Zhongyu Zhou, Wendy Sanchez, Xiaoyu Che, and the URP program for their dedication and willingness to help me realize this ambitious 2-year project.





Jessica Chun  
Bioengineering  
Junior

LAB NAME  
**Annabi Lab**

FACULTY ADVISOR  
**Nasim Annabi**

GRADUATE STUDENT DAILY LAB SUPERVISOR  
**Sevana Baghdasarian**

DEPARTMENT  
**Chemical Engineering**

## Electrospun polycaprolactone (PCL) and gelatin-methacryloyl (GelMA) scaffold for urethral extension in a rabbit model

Tissue engineering combines cells, scaffolds, and biochemical factors in a way that is capable of regenerating biological tissue and organs. Many studies have been done on the regeneration of skin, bone, and cartilage. However, there are limited studies on urethra tissue engineering. The goal of this study is to engineer an electrospun polycaprolactone (PCL) and gelatin methacryloyl (GelMA) scaffold that is mechanically similar to native urethral tissue and test it in vivo using a rabbit model. By electrospinning the GelMA/PCL polymer (dissolved in Hexafluoroisopropanol (HFIP)), the scaffold resembles certain properties of the extracellular matrix (ECM), allowing for cell adhesion and migration. By altering the GelMA/PCL ratio, mechanical and degradation properties are optimized to provide a comparable elasticity to the urethral tissue. In further studies, a tubular scaffold will be formed, mechanically tested, and seeded with urothelial and smooth muscle cells creating a biomimetic scaffold for urethra tissue regeneration. The tubular scaffolds will eventually aid in a more consistent and less invasive procedure for urethroplasties, eliminating the need to use an autograft for the reconstruction of the damaged urethra.

# Electrospun Polycaprolactone (PCL) and Gelatin-Methacryloyl (GelMA) Scaffold for Urethral Tissue Regeneration

Jessica Chun<sup>1</sup>, Sevana Baghdasarian<sup>1</sup>, Renea Sturm<sup>2</sup>, Brian Walker<sup>1</sup>, and Nasim Annabi<sup>1</sup>  
<sup>1</sup>University of California Los Angeles (UCLA) Samueli School of Engineering Department of Chemical and Biomolecular Engineering  
<sup>2</sup>David Geffen School of Medicine at UCLA, Department of Urology

UCLA Samueli School of Engineering | UNDERGRADUATE RESEARCH PROGRAM | UCLA Engineering Chemical and Biomolecular Engineering | UCLA Health

### ABSTRACT

Tissue engineering combines cells, scaffolds, and biochemical factors in a way that is capable of regenerating biological tissue and organs. Many studies have been done on the regeneration of skin, bone, and cartilage. However, there are limited studies on urethra tissue engineering. The goal of this study is to engineer an electrospun polycaprolactone (PCL) and gelatin methacryloyl (GelMA) scaffold that is mechanically similar to native urethral tissue and test it in vivo using a rabbit model. By electrospinning the GelMA/PCL polymer (dissolved in Hexafluoroisopropanol (HFIP)), the scaffold resembles certain properties of the extracellular matrix (ECM), allowing for cell adhesion and migration. By altering the GelMA/PCL ratio, mechanical and degradation properties are optimized to provide a comparable elasticity to the urethral tissue. In further studies, a tubular scaffold will be formed, mechanically tested, and seeded with urothelial and smooth muscle cells creating a biomimetic scaffold for urethra tissue regeneration. The tubular scaffolds will eventually aid in a more consistent and less invasive procedure for urethroplasties, eliminating the need to use an autograft for the reconstruction of the damaged urethra.

### BACKGROUND & MOTIVATION

**What is Hypospadias?**

It is a congenital condition in which the opening of the urethra is on the underside of the penis instead of at the tip. In some cases, it results in anomalous penile development, ventral penile curvature, and hooded foreskin.

**~1:250**  
Males with Hypospadias

Currently, urethroplasties use penile skin flaps or buccal mucosa grafts to fix the injured or excised urethra. Although this is a reasonable solution, there are still high reoperation rates after the first fixation procedure. My project aims to combine GelMA and PCL, polymers that have each previously been used in medical devices, to create a scaffold that will sufficiently model the urethra. Previous studies have shown GelMA/PCL scaffolds being used for vascular tissue engineering, but not for urethra tissue engineering.

**Complications Resulting in Reoperation**

**Fistula:** an abnormal passage  
**Diverticulum:** expansion of a weak point in the tract, forming a sac  
**Dehiscence:** the splitting or bursting open of a pod or wound

**Rate of Reoperation for proximal hypospadias cases**  
 → 49-68% (Gong 2017)

### NATIVE TISSUE CHARACTERIZATION

Recorded width, length (gauge length), and thickness, then ran the test at 10 mm/min until the sample broke. The elastic modulus (slope) was calculated from the stress-strain curve.

Measures:  
 → speed  
 → force (stress)  
 → distance (strain)

### POLYMER PREPARATION

**GelMA**

- Made from gelatin, a denatured form of collagen (modified natural ECM component)
- Has natural cell binding motifs (RGD) that enhance cell adhesion
- Photopolymerizable
- Tunable mechanical properties
- Biodegradable

**Polycaprolactone**

- Low melting temperature, so easy to manipulate
- Biodegradable
- Biocompatible
- Cost-effective

The process involves GelMA synthesis, PCL synthesis, and their combination in a solvent (Hexafluoroisopropanol) followed by electrospinning and crosslinking with a photoinitiator (Irgacure dissolved in ethanol) under UV light to create a crosslinked scaffold with GelMA & PCL nanofibers.

### ELECTROSPINNING THE SCAFFOLD

**Our Setup**

- 1 ml/hr flow rate
- 12 cm distance
- 25 kV
- 18 Gauge syringe

**Electrospinning**

A process that charges droplets of polymer and results in creating a mat of nanofibers that is highly porous and has high surface area (good for cell environment and similar to ECM)

**Complications**

- Uniformity
- Unsticking scaffold from aluminum surface

### FUTURE EXPERIMENTS

- Create different % w/v polymer solutions
  - 10% w/v GelMA/0% w/v PCL (shown to the left), 10% w/v GelMA/10% w/v PCL, 10% w/v GelMA/20% w/v PCL, etc.
- Conduct tensile tests on the different concentrated GelMA/PCL scaffolds, which were prepared in HFIP.
- Conduct compression and burst pressure tests to characterize the native tissue and scaffold more
- Electrospin a tubular shaped scaffold directly on a spinning mandrel

### REFERENCES AND ACKNOWLEDGEMENTS

Qiang, E.M. and Cheng, E.Y. (2017). Current challenges with proximal hypospadias: We have a long way to go. *J. Pediatr. Surg.* 52(10):207-209.

Li, T. C. and Yu, J. and Tan, W. S. (2015). Gelatin methacrylate (GelMA) methacrylate hydrogels with tunable modulus for controlled drug release. *Journal of Materials Chemistry B* 4, 13, 2264-2273.

Patel, P. and K. S. (2017). Electrospinning of Gelatin Nanofibers Using Different Protocols. *Journal of Materials Science* 42, 2183-2193. 10.1007/s10853-017-1381-2

Shimoda, M. et al. (2016). Precise Tuning of Gelatin-PCL Composite Nanofiber (GelMA) Synthesis. *Scientific Reports* 6, 21038.

<https://doi.org/10.1038/s41598-016-06398-9>

<https://www.ncbi.nlm.nih.gov/pmc/articles/PMC5010000/>

<https://www.researchgate.net/publication/315000000>

This work is supported by the National Institutes of Health (NIH GM55052).

I would also like to acknowledge the Annabi Lab and the Undergraduate Research Program at the University of California Los Angeles (UCLA) Samueli School of Engineering.



Ashley Dickman  
Bioengineering  
Junior

LAB NAME

Annabi Lab

FACULTY ADVISOR

Nasim Annabi

GRADUATE STUDENT DAILY LAB SUPERVISOR

Brian Walker

DEPARTMENT

Chemical Engineering

## Synthesis and Characterization of Elastin-like Polypeptides (ELPs) and Gelatin-Methacryloyl (GelMA) Hydrogels for Lung Sealant Application

Sutures and staples are currently the conventional method for lung repair, but these techniques are associated with secondary tissue trauma, and infections. Instead of these two methods, we developed an adhesive and elastic hydrogel that may be used as a lung sealant. As a surgical sealant, we synthesized hydrogels with varying concentrations of proteins gelatin methacryloyl (GelMA) and elastin-like polypeptide (ELP). GelMA is a chemically modified form of gelatin that exhibits robust mechanical and biodegradation properties, and has the ability to support cell adhesion via RGD peptide sequences. ELP is a modified form of the extracellular matrix protein elastin. I specifically aimed to characterize the degradation profiles, swelling properties, and burst pressure using an ex vivo porcine lung model of these hydrogels. These experiments showed the ability to optimize the degradation of the hydrogels based on concentration and to adhere to lung tissue while holding air pressure from mechanical ventilation. This ELP-GelMA hydrogel has the potential of surgical applications with its ability to impart different properties that may closely mimic those of native tissues decreasing secondary tissue trauma and allowing for tissue recovery.



## Synthesis and Characterization of Elastin-like Polypeptides (ELPs) and Gelatin-Methacryloyl (GelMA) Hydrogels for Lung Sealant Application

UCLA Samueli School of Engineering

Ashley Dickman<sup>1</sup>, Brian Walker<sup>2</sup>, and Nasim Annabi<sup>2</sup>

<sup>1</sup>Department of Bioengineering, UCLA, <sup>2</sup>Department of Chemical and Biomolecular Engineering, UCLA

UNDERGRADUATE RESEARCH PROGRAM

### Abstract

Sutures and staples are currently the conventional method for lung repair, but these techniques are associated with secondary tissue trauma, and infections. Instead of these two methods, we developed an adhesive and elastic hydrogel that may be used as a lung sealant. As a surgical sealant, we synthesized hydrogels with varying concentrations of proteins gelatin methacryloyl (GelMA) and elastin-like polypeptide (ELP). GelMA is a chemically modified form of gelatin that exhibits robust mechanical and biodegradation properties, and has the ability to support cell adhesion via RGD peptide sequences. ELP is a modified form of the extracellular matrix protein elastin. I specifically aimed to characterize the degradation profiles, swelling properties, and burst pressure using an ex vivo porcine lung model of these hydrogels. These experiments showed the ability to optimize the degradation of the hydrogels for surgical applications based on concentration and to adhere to lung tissue while holding air pressure from mechanical ventilation.

### Background

**Goal: Photocrosslinkable Hydrogel as Sealant Material**

- Hydrogel acts as a scaffold platform for tissue engineering
- Mimic the native tissue of the lung
- Degrade within a certain time frame to allow cell proliferation
- Use crosslinking for strong mechanical properties
- Hold a high enough burst pressure so no air leakage from initial incision

### Materials & Methods

**ELP Synthesis**

- Mimic extracellular matrix

**GelMA Synthesis**

- Derived from collagen

**Hydrogel Preparation**

Combine different concentrations of components

Pipet 70  $\mu$ l into PDMS Mold

Photopolymerization

### Porcine Ex-vivo Lung Incision Model

- Cut incision into lung to model surgical lobectomy
- Apply composite hydrogel and photo crosslink
- Using ventilator and pressure sensor, get measurements for at which the sealant holds
- Porcine lung is placed in a water bath to determine burst pressure

Depending on the concentration of ELP, the burst pressure will differ. At burst pressure, the sealant no longer holds and will release air.

**Hydrogel Degradation**

Weigh crosslinked lyophilized hydrogel samples

Incubate each sample with collagenase

Weigh at different time points for degradation percentages

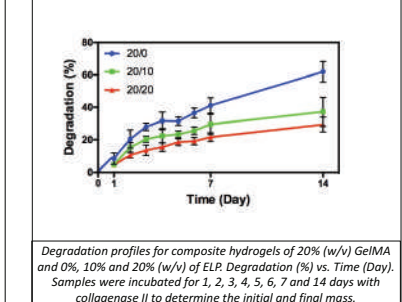
**Hydrogel Swelling Analysis**

Weigh crosslinked lyophilized hydrogel samples

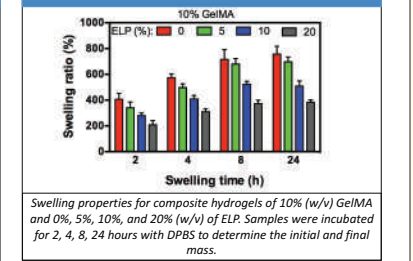
Incubate each sample with DPBS

Weigh at different time points for swelling ratio

### Degradation Profiles



### Swelling Properties



### Conclusions

- This work demonstrates a method of ELP-GelMA composite, photocrosslinkable hydrogel as a surgical sealant
- GelMA is derived from collagen, so as a natural polymer it is able to degrade more easily than ELP
- ELP has high hydration properties that allow for swelling
- Different concentrations of ELP vs. GelMA in a hydrogel allow the properties to be tunable depending on the surgical application
- Able to change the optimal timeframe of hydrogel in the body based on concentration of ELP
- As a lung sealant, with high burst pressure it can seal air flow and keep function of organ to allow mobility

### Future Directions

- Testing different properties of the hydrogel including biocompatibility, mechanical and adhesive properties to get a holistic results of the hydrogel in-vitro
- Applying and tailoring this hydrogel to different types of tissue in the body by changing degradation, swelling, burst pressure properties, etc.
- In-vitro studies of the surgical sealant on a porcine lung

### References & Acknowledgments

Elhademoussini, A., Langer, R., Borenstein, J. & Vacanti, J. P. Microscale technologies for tissue engineering and biology. *Proc. Natl. Acad. Sci. U. S. A.* **103**, 2480-2487 (2006).

Pedersen, T. B. et al. Comparative Study of Lung Sealants in a Porcine Ex Vivo Model. *ATIS* **94**, 234-240 (2012).

B Hutson, C. et al. Synthesis and Characterization of Tunable Poly(Ethylene Glycol)-Gelatin Methacrylate Composite Hydrogels. *Tissue Engineering, Part A* **17**, (2011).

Tamayol, A., Annabi, N. & Khademhosseini, A. Biomaterials Synthesis, properties, and biomedical applications of gelatin methacryloyl (GelMA) hydrogels. *Biomaterials* **73**, 254-271 (2015).

Thank you to the Annabi Lab at UCLA Samueli School of Engineering and UCLA Samueli Engineering Undergraduate Research Program.



Adrien Hadj-Chaib  
Computer Science  
Junior

LAB NAME  
**Computer Graphics and Vision Laboratory**

FACULTY ADVISOR  
**Demetri Terzopoulos**

GRADUATE STUDENT DAILY LAB SUPERVISOR  
**Masaki Nakada**

DEPARTMENT  
**Computer Science**

## Autonomous Bipedal Deceleration using Reinforcement Learning

Reinforcement Learning is learning through trial and error. An agent, here a humanoid 3D model, interacts in a physics based environment by taking actions, producing some torques to move its articulations. A feedback reward from the environment is then observed by the agent after taking an action. The agent will learn to optimize its actions to maximize its long term accumulated reward. In this case, if we use a reward that encourages the model to stay upright, on its two legs, and move at a certain velocity, the model will effectively learn to walk starting from rest. The power of this method is that the agent doesn't need to be shown how to walk, and can learn how to if provided with a good enough reward function. Previous works managed to make a model walk with varying degrees of realistic and noisy movements. However, the previous implementations have in common that the model starts from rest and accelerates until reaching a set target velocity, and then maintains that velocity until falling off. The goal of my work has been to take one such implementation and modify it in order to make the humanoid model learn how to decelerate to a resting position without losing balance. This has been done using a piece-wise policy method, which decomposes the movement into an acceleration and a deceleration phase. Although this method enables the model to successfully learn deceleration, the resulting motion is very inconsistent and the model often falls off prematurely.



## Autonomous bipedal deceleration using Reinforcement Learning



Undergraduate  
Research  
Program

Adrien Hadj-Chaib<sup>1</sup>, Masaki Nakada<sup>1</sup>, Demetri Terzopoulos<sup>1</sup>  
<sup>1</sup>Department of Computer Science, University of California, Los Angeles  
Computer Graphics and Vision Laboratory

### 1. Abstract

Reinforcement Learning is learning through trial and error. An agent, here a humanoid 3D model, interacts in a physics-based environment by taking actions, producing some torques to move its articulations. A feedback reward from the environment is then observed by the agent after taking an action. The agent will learn to optimize its actions to maximize its long-term accumulated reward. In this case, if we use a reward that encourages the model to stay upright, on its two legs, and move at a certain velocity, the model will effectively learn to walk starting from rest. The power of this method is that the agent doesn't need to be shown how to walk and can learn how to if provided with a good enough reward function. Previous works managed to make a model walk with varying degrees of realistic and noisy movements. However, the previous implementations have in common that the model starts from rest and accelerates until reaching a set target velocity, and then maintains that velocity until falling off. The goal of my work has been to take one such implementation and modify it in order to make the humanoid model learn how to decelerate to a resting position without losing balance [1]. This has been done using a piece-wise policy method, which decomposes the movement into an acceleration and a deceleration phase. Although this method enables the model to successfully learn deceleration, the resulting motion is very inconsistent and the model often falls off prematurely.

### 2. Reinforcement Learning



The Agent takes actions following a policy function  $\pi(a_t | S_t) = \pi(a_t | S_{t-1})$

Goal: Learn the optimal policy  $\pi^*$  which maximizes the accumulated reward R by always picking the best possible action a

Training: Interacting with the environment to learn  $\pi^*$ , which maximizes the accumulated reward R

Evaluation: Let the model act a sequence of states, resulting in a motion trajectory, by following its learned policy  $\pi^*$

### 3. Materials

The Reinforcement Learning Algorithm to train the 3D model was set with the following parameters:

Action:  $a =$  torque actuated at each articulated joint

State:  $S = [q, \dot{q}, c, v]$ , with

- $q$  the joint positions
- $\dot{q}$  the joint velocities
- $c$  an indicator of contact between the end effectors and the ground
- $v$  the target velocity of the Agent's center of mass in the forward direction

Reward:  $r(s,a) = w_v E_v(s) + E_c(s) + w_e E_e(s) + E_s + w_e E_e(a)$ , with

- $w_v$  the weight applied to the velocity component of the reward
- $E_v(s)$  reward for being closer to the target velocity
- $E_c(s)$  reward for maintaining the torso and head upright
- $w_e$  the weight applied to the alignment with the forward direction
- $E_e(s)$  reward for staying in the forward direction
- $E_s$  reward for staying alive, not lose balance
- $w_e$  the weight applied to the minimal joint usage
- $E_e(a)$  reward for not using excessive joint force

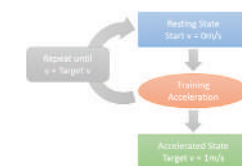
The symmetrical component of the motion is set in place by adding another term to the policy function  $\pi$  which encourages the Agent to take symmetrical actions. The Agent focuses on taking symmetrical actions rather than trying to achieve a symmetry of posture.

Hence, the Agent is inclined to walk at the desired velocity starting from rest, while keeping an upright position and without losing balance. For a more realistic motion, the model was also encouraged to take symmetric actions and not use excessive joint force.

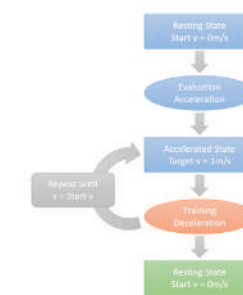
### 4. Methods

The focus of my approach to learn deceleration is to use a piece-wise policy. Rather than using a complex policy that would be able to walk at any velocity, I decided to use two different simpler policies.

The first policy is the acceleration policy, which has the objective to start from rest and accelerate to reach and move at the target velocity.



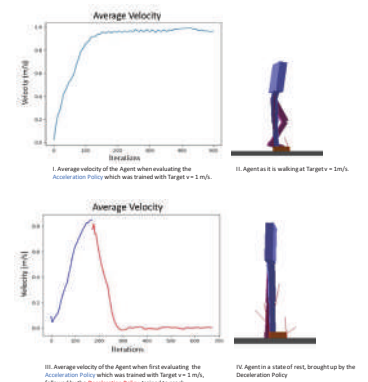
The second policy is the deceleration policy, which has the objective to start from a state of motion at the target speed and decelerate to a state of rest and stay upright.



Once both acceleration and deceleration policies have been trained, we can evaluate them sequentially to generate an accelerating then decelerating motion trajectory.



### 5. Results



### 6. Conclusion

Advantages of the piece wise policy:

- Achieved learning a deceleration motion which resulted to an Agent coming to a full stop without losing balance.
- Can generalize to running and walking backwards.
- Theoretically intuitive, could build a piece wise controllable character.

Drawbacks of the piece wise policy:

- Model is unstable in evaluation and often falls off prematurely.
- Model walks straight ahead, no possibility to turn

### 7. References

[1] Wenhao Yu, Greg Turk, and C.Karen Liu. 2018. Learning Symmetric and Low-Energy Locomotion. ACM Trans. Graph. 37, 4, Article 144 (August 2018), 12 pages. <https://doi.org/10.1145/3197517.3201397>



Omar Issa  
Civil and Environmental  
Engineering  
Senior

LAB NAME  
**Next-Generation Liquefaction Working Group**

FACULTY ADVISOR  
**Jonathan P. Stewart**

DAILY LAB SUPERVISOR  
**Paolo Zimmaro**

DEPARTMENT  
**Civil and Environmental Engineering**

## Developing Sites with Variable Performance for the Next-Generation Liquefaction (NGL) Case History Database

Earthquake-induced liquefaction typically occurs in loose saturated sandy soils that, under the cyclic loading imposed by the earthquake, experience a sudden loss in strength. This phenomenon can cause major destruction and loss of life. Current models used to evaluate liquefaction hazard are either purely empirical or semi-empirical, hence heavily reliant on case history data. The Next-Generation Liquefaction (NGL) database is a global research project with the aim of substantially improving quality, transparency, and accessibility of case history data related to liquefaction. Most field observations in NGL sites to date include widespread liquefaction manifestation or no manifestation at all – this necessitated the development and testing of an NGL case history wherein a single site experienced variable performance. This unique scenario was observed in Wufeng, Taiwan (Site A) after the 1999 Chi-Chi Earthquake, wherein the western half of the site suffered extensive ground failure and structural damage while the eastern portion experienced no observable surface evidence of ground failure. Using test data extracted from the Pacific Earthquake Research Center's (PEER) Taiwan Ground Failure Database and written field observations detailed in Chu et. al (2004), an NGL case history was successfully developed and uploaded to the database. In addition to providing a framework for sites with variable performance, data from this case history will be used to develop new liquefaction susceptibility and triggering models in the future.

Samueli  
School of Engineering

UNDERGRADUATE RESEARCH PROGRAM

US NRC MPC LIDOT

### Developing Case Histories with Variable Performance for the Next-Generation Liquefaction (NGL) Database

Research Advisors: Paolo Zimmaro, Jonathan P. Stewart  
Department of Civil & Environmental Engineering, University of California, Los Angeles

---

Induced liquefaction, which occurs when saturated sandy soils experience a sudden loss in strength, can cause major destruction and loss of life.

Generation Liquefaction (NGL) database is a global research project with the aim of substantially improving quality, transparency, and accessibility of case history data related to ground failure. Since the completion of the NGL database structure in 2018, extensive testing has been performed by the database working group. Most field observations in NGL sites to date include widespread liquefaction manifestation or no manifestation at all – this necessitated the development and testing of an NGL case history wherein a single site experienced variable performance.

**What is an NGL Case History?**

An NGL case history consists of three parts: (1) geotechnical/geological site characterization, (2) observed field performance, including evidence of liquefaction, ground failure, or non-earthquake event/ground motion information, liquefaction after the 1964 Niigata Earthquake in Japan. (Photo from NOAA)

**Selected NGL Case History**

Wufeng, Taiwan (Site A), 1999 Chi-Chi

Locations of field tests at Wufeng Site A (left) and aerial imagery of the site with the western and eastern portions boxed in different colors (right).

During the early hours of September 21, 1999, a magnitude 7.6 M struck central Taiwan, instantly making it the largest earthquake in the country disaster reconnaissance mission was sponsored by the Pacific Earthquake Engineering Research (PEER) Center, with field work performed primarily in two locations: Wufeng and Nantou, Taiwan.

Site A was among five different sites studied in Wufeng. Located in the southern portion of city, the site exhibited a drastic range of ground performance. Multi-story reinforced concrete buildings on the western half of the site experienced extensive structural damage, differential settlement, foundation punching failures, and full foundation-bearing failures. Single-story buildings on the eastern end of the site experienced no observable evidence of ground failure. The unique conditions observed at Site A motivated the development of NGL case history.

Evidence of severe structural damage and ground failure on the west side of the site (Photo: R. Seed, 1999). These photos are uploaded as associated files for the case history.

Photography depicting the lack of ground failure near residential units on the eastern end of the site. (Photo: R. Seed, 1999)

---

Upon uploading the template to database, all relevant data for the case history will be made available on the NGL user interface, which hosts a number of useful tools for interaction with the data.

The NGL interface allows users to interact with the data either in list view (left) or map view (right). Using either method, users can readily access the locations where ground failure occurred, along with written descriptions and associated files. While the map view offers more information about the relative locations of field tests and observations, the list view allows users to download relevant associated files with ease.

After distilling all relevant information associated with Wufeng Site A, the data was organized in an Excel template created for the NGL database.

The NGL template follows the database schema, which contains 53 tables and four main sections. The following diagram summarizes a few of the major tables.

Site data used to characterize Wufeng Site A includes field test data, sample data, index test data, stratigraphy data as well as associated files.

Field test data associated with Wufeng Site A was primarily sourced from subsurface investigations performed in 2001 and 2002 by a PEER investigation included Standard penetration tests (SPT) with rotary wash, cone penetration tests (CPT) with cone tip resistance (CPT) and cone sleeve friction (CSF) data.

Boring logs with SPT (left) and CPT data files (right) were distilled from their original formats into an NGL template for inclusion in the database. While CPT data was often digitized, SPT data required a more rigorous distillation procedure involving manual interpretation and digitization of each boring log.

3: Earthquake Event / Ground Motion Data

Earthquake event information currently available in the NGL database was extracted from the Next Generation Attenuation databases, NGA West and NGA Subduction. This data is uploaded and maintained by a small group to ensure proper coordination between the NGL and NGA databases. To associate the 1999 Chi-Chi Earthquake and relevant ground motion data with this case history, the earthquake was simply selected prior to uploading the case history.

---

A case history for Wufeng Site A was successfully developed for NGL after a rigorous distillation process involving 13 field tests and the organization of over 75 associated files. This process is well documented and can provide a framework for developing case histories for sites with variable performance.

In addition, Site A has been used extensively in the past for liquefaction model development. As an NGL case history, it will be available for use by researchers who wish to develop new liquefaction susceptibility and triggering models in the future.

**References and Acknowledgements**

I would like to acknowledge my mentor, Paolo Zimmaro and my faculty advisor, Professor Stewart for their support and encouragement. I would also like to extend my thanks to the Samueli Engineering Undergraduate Research Program.



Alexis Joo  
Materials Engineering  
Junior

LAB NAME  
**Di Carlo Laboratory**

FACULTY ADVISOR  
**Dino Di Carlo**

GRADUATE STUDENT DAILY LAB SUPERVISOR  
**Joe de Rutte**

DEPARTMENT  
**Bioengineering**

## Dynamics of Droplets Templated by 3D Millimeter Scale Particles

An emulsion is a mixture of two immiscible liquids that is found anywhere from the morning cup of milk (or cream in coffee) to cosmetic creams to micro-scale compartments for biomolecules and cells. Individual droplets within an emulsion system are typically stabilized by hydrophilic and hydrophobic molecules called surfactants, which form a thin layer between the two immiscible liquids. Although this approach is suitable for short term applications, the surfactant-stabilized droplets are metastable, meaning they will eventually coalesce over time to reach their thermodynamic equilibrium. Recently, we developed armoured emulsions which utilized 3D-structured microparticles to stabilize individual droplets. These drop-carrier-particles have an inner hydrophilic layer to capture and stabilize water droplets, and an outer hydrophobic layer to disperse the particles in oil and act as a barrier to coalescence. In contrast to typical emulsions, these armored emulsions have a local energetic minima which enables long term stability and controls the volume in each particle droplet. In order to further understand the mechanics of this system, millimeter scale particle droplets were fabricated using 3D printing and tested in PPG (an oil phase). The millimeter-scale version demonstrated stabilize monodisperse water droplets which agrees with both microscale experiments and simulations. In future work this millimeter-scale platform will be used to elucidate fundamental theories surrounding the physics of this new class of emulsions.



### Dynamics of Droplets Templated by 3D Millimeter Scale Particles

Alexis Joo<sup>1</sup>, Joseph de Rutte<sup>2</sup>, Chueh-Yu Wu<sup>2</sup>, Bao Wang<sup>3</sup>, Kyung Ha<sup>3</sup>, Andrea L. Bertozzi<sup>3,4,5</sup>, and Dino DiCarlo<sup>2,4,5,6</sup>

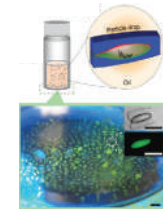
<sup>1</sup>Materials Engineering Department, <sup>2</sup>Bioengineering Department, <sup>3</sup>Mathematics Department, <sup>4</sup>Mechanical and Aerospace Engineering Department, <sup>5</sup>California NanoSystems Institute (CNSI), <sup>6</sup>Jonsson Comprehensive Cancer Center, University of California, Los Angeles, CA 90025 USA



---

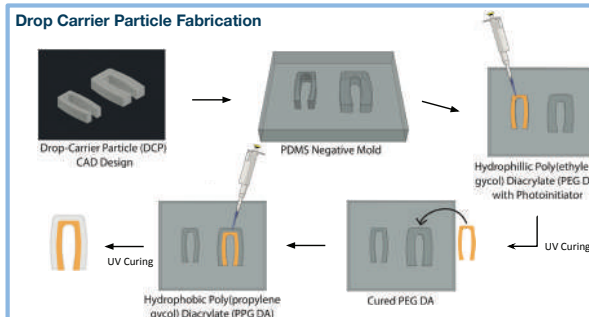
#### Introduction

- Emulsion is the mixture of two immiscible liquid
  - Salad Dressing: shake to emulsify
  - Milk (milk fat-in-water): milk protein act as emulsifier
  - Face cream (oil and water): chemical surfactant act as emulsifier
  - Drug/Vaccine delivery: compartment for biomolecules and cells
- Standard emulsions are metastable
  - Degrades/coalesce with time
- 3D-structured microparticles "armoured emulsions"
  - Hydrophilic inner layer
  - Hydrophobic outer layer
  - Stable, monodisperse
- Millimeter scale drop-carrier particles using 3D printed molds
  - Study dynamics of particle drop formation
  - Model the phenomenon in micrometer scale using dimensionless parameters



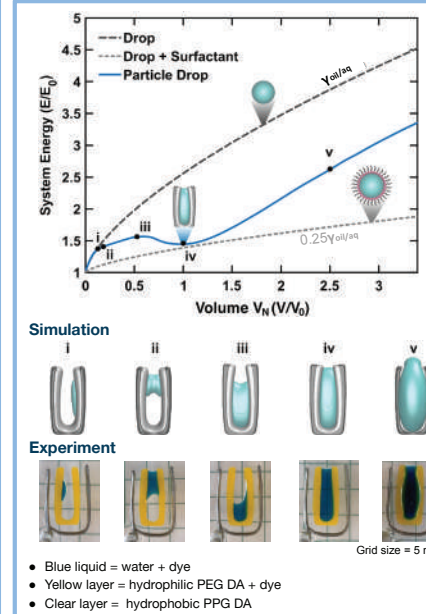
#### Materials and Methods

##### Drop Carrier Particle Fabrication



---

#### Particle-Drop Formation



**Simulation**

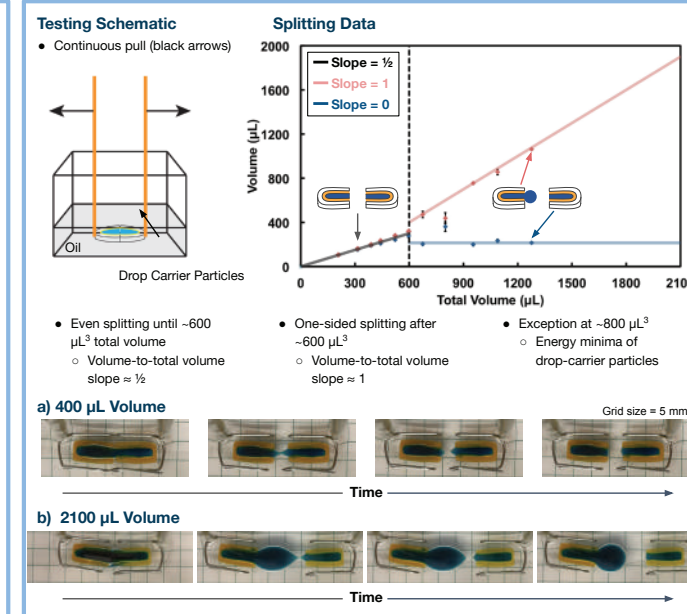
**Experiment**

- Blue liquid = water + dye
- Yellow layer = hydrophilic PEG DA + dye
- Clear layer = hydrophobic PPG DA

#### Water Splitting in Particles

Testing Schematic: Continuous pull (black arrows) through a channel containing oil and drop-carrier particles.

##### Splitting Data



- Even splitting until ~600 μL<sup>3</sup> total volume
  - Volume-to-total volume slope ≈ 1/2
- One-sided splitting after ~600 μL<sup>3</sup>
  - Volume-to-total volume slope ≈ 1
- Exception at ~800 μL<sup>3</sup>
  - Energy minima of drop-carrier particles

**a) 400 μL Volume**

**b) 2100 μL Volume**

Grid size = 5 mm

---

#### Conclusions

- Water encapsulated inside a single milli-scale drop-carrier particle is **stable** (energetic minima)
- Drop-carrier particles create **monodisperse droplets** by splitting up larger volumes of water

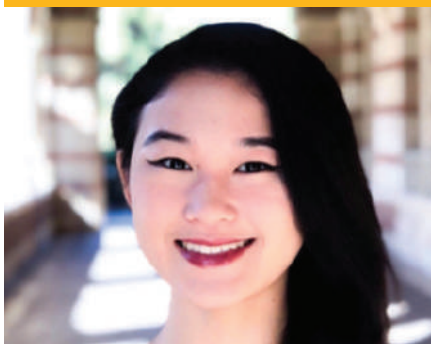
#### Future Plans

- Explore different drop-carrier particle geometries to find optimal shapes for stable, monodisperse droplet formation

#### Acknowledgements

I thank the UCLA Undergraduate Research Program, PATHS-UP for their funding and support.





Kayli Masuda  
Chemical Engineering  
Freshman

LAB NAME  
**Park Lab**

FACULTY ADVISOR  
**Jun Park**

GRADUATE STUDENT DAILY LAB SUPERVISOR  
**Jimmy Xu**

DEPARTMENT  
**Chemical Engineering**

## Optimizing Carbon Dioxide to Ethanol Conversion via the Symbiotic Metabolism of a Yeast and Cyanobacteria Co-culture

In the quest for energy independence, it is key to develop sustainable technologies for renewable energy. Simultaneously, carbon fixation is essential to reducing the atmospheric carbon dioxide contributing to rising global temperatures. One such technology that addresses both of these environmental concerns is the metabolic engineering of photosynthesis and fermentation. Photosynthetic cyanobacteria convert carbon dioxide to glucose while fermenting yeast converts glucose to ethanol and carbon dioxide. The co-dependent nature of these bioprocesses creates the opportunity to co-culture these organisms, producing a symbiotic system in which ethanol is the net product. Thus, this project investigates the growth rate of yeast to find metabolic controls and determine whether ethanol optimization is a viable application.

First, inoculums of the yeast *S. cerevisiae* BY 4742 and the cyanobacteria *S. elongatus* WT 7942 were isolation streaked to produce individual colonies. An individual colony of yeast was cultured with or without cyanobacteria in solutions of varying carbon sources and growth media, which were stored in a shaking incubator at 30°C. By monitoring optical density with the spectrophotometer over a week, the growth rate for each solution was found. The data appears to show that YNB/BG-11 is the preferential growth media and that a co-culture with cyanobacteria significantly improves the growth rate of yeast. Future work will use HPLC and YSI analyzers to quantify nutrient consumption and production secretion.

## Optimizing Carbon Dioxide to Ethanol Conversion via the Symbiotic Metabolism of a Yeast and Cyanobacteria Co-culture

Kayli Masuda and Jun Park

Chemical and Biomolecular Engineering Department, University of California, Los Angeles

**UCLA Samueli**  
School of Engineering

UNDERGRADUATE RESEARCH PROGRAM

### Introduction

- In the quest for energy independence, it is key to develop sustainable technologies for renewable energy. Simultaneously, it is of paramount importance to reduce the atmospheric carbon dioxide contributing to rising global temperatures.
- One technology that addresses both of these environmental concerns is metabolic engineering. Metabolic engineering is the field of optimizing specific chemical reactions in biological organisms.
- For example, photosynthetic cyanobacteria convert carbon dioxide to glucose while fermenting yeast converts glucose to ethanol and carbon dioxide. The co-dependent nature of these bioprocesses creates the opportunity to co-culture cyanobacteria and yeast, producing a symbiotic system in which ethanol is the net product.

### Current Knowledge

- The current field of knowledge for yeast and cyanobacteria as separate organisms is extensive e.g. their optimal growth conditions, their metabolic reactions, and their potential applications in industry.
- In contrast, there is only one notable article researching a co-culture of yeast and cyanobacteria, which used a biotechnology approach to explore lipid production.<sup>1</sup>
- Therefore, this project aims to further investigate this topic by using a metabolic engineering approach with the goal of ethanol production.

### Experimental Design

- Approach**
- I will investigate the growth rate of yeast when cultured with and without cyanobacteria in variations of carbon source and growth media.

No.	Organism(s)	Carbon Source	Growth Media
1	Yeast	Glucose	YNB
2	Yeast	Glucose	BG-11
3	Yeast	Acetic Acid	BG-11
4	Yeast	Glucose	YNB/BG-11
5	Yeast and Cyanobacteria	Glucose	YNB/BG-11
6	Yeast and Cyanobacteria	Acetic Acid	YNB/BG-11

**Table 1. Experimental Design.** For the organisms, yeast strain *Saccharomyces cerevisiae* BY 4742 and cyanobacteria strain *Synechococcus elongatus* WT (wild type) 7942 were used. For the yeast carbon source, glucose and acetate were in concentrations of 0.4 grams per liter. For the media, 1X Yeast Nitrogen Base (YNB) without amino acid additives and "Blue-Green algae" media 11 (BG-11) with 50 millimolar sodium bicarbonate were used.

### Rationale:

- Experiments (exp.) 1, 2, and 4 controls carbon source to test yeast growth in variations of media e.g. yeast's YNB media, cyanobacteria's BG-11 media, and a combination of the two.
- Exp. 2 and 3 hold media constant to test yeast growth in two carbon sources e.g. glucose and acetic acid.
- Exp. 4 serves as a control for exp. 5 and 6, which test yeast growth in a co-culture with cyanobacteria on two differing carbon sources e.g. glucose and acetic acid.

### Methods

#### Preparation of organisms

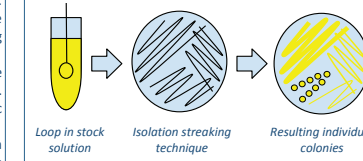


**Figure 1.** An inoculum of the yeast and cyanobacteria strains were each streaked for isolation using an inoculation loop, resulting in individual colonies.

#### Preparation of medias

Following "Table 1. Experimental Design," the correct carbon source and growth media were combined create 50 mL each of the six experimental variations.

#### Culturing organism into media

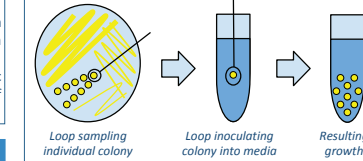


**Figure 2.** Inoculation loop inoculates, or transfers, an individual colony into the prepared media, in which it will grow for a week in a shaking incubator at 30° Celsius.

#### Growth Rate via Optical Density (OD)

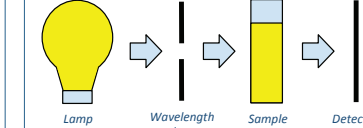


**Figure 3.** In a spectrophotometer, light from a lamp first passes through a wavelength selector. Then, the selected wavelength of light passes through the sample until it reaches a detector. The natural log of the detected number is called optical density (OD), an indicator of exponential cell growth. Measurements of OD were taken every other day for a week, forming a linear trend line with the growth rate as the slope.

### Acknowledgements

I would like to thank Dr. Jun Park for kindly providing his conceptual ideas, support, and lab space. I would also like to thank Ph.D. candidate Derrick Chuang for providing the cyanobacteria. Lastly, thank you to the UCLA Samueli Engineering Undergraduate Research Program for improving my technical writing and presentation skills.

### Reference

- Biotechnology for Biofuels*, 2017, Volume 10, Number 1, Page 1. Tingting Li et. Al.

### Results

#### Experiments 1 – 4: Yeast Growth

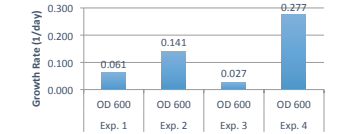


**Table 2. Experiments 1 – 4: Yeast Growth.** Exp. 1 and 2 show that BG-11 unexpectedly outperformed YNB media. Exp. 2 and 3 show that glucose outperforms acetic acid. Exp. 4 shows that YNB/BG-11 media outperforms either component alone.

#### Experiment 5: Co-culture with glucose

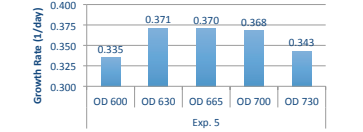


**Table 3. Experiment 5: Co-culture with glucose.** The optimal wavelengths to measure optical density are 600 nanometers (nm) and 730 nm for yeast and cyanobacteria respectively. Thus, the bell-like curve formed by this range of wavelengths demonstrates a balanced co-culture. The co-culture appears to have improved yeast growth by 150%, from 0.277 (Table 2. Exp. 4) to 0.335 day<sup>-1</sup>.

#### Experiment 6: Co-culture with acetic acid

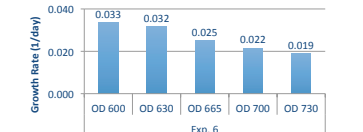


**Table 4. Experiment 6: Co-culture with acetic acid.** With growth rate decreasing from yeast's 600 nm wavelength to cyanobacteria's 730 nm, the results show an unbalanced co-culture dominated by yeast. However, the co-culture still appears to have improved yeast growth by 120%, from 0.027 (Table 2. Exp. 3) to 0.033 day<sup>-1</sup>.

### Conclusion

#### Hypothesis revisited and contributions:

- For carbon source, glucose is preferred over acetic acid. For growth media, YNB/BG-11 is preferred over BG-11, which outperforms YNB. Thus, this work contributes two types of metabolic control for yeast growth and renders YNB unnecessary for future experiments.
- The growth rate of yeast appears to have significantly improved via a co-culture with cyanobacteria. This supports the optimization of ethanol production and implies greater applications of co-cultures to a variety of co-dependent organisms.

#### Future Experiments and Progress

- High-performance liquid chromatography (HPLC) and the Yellow Springs Instrument (YSI) analyzer will quantify nutrient consumption and product secretion to confirm these preliminary results.
- Further variations of carbon source and growth media will be tested e.g. glucose with BG-11 media alone.



Manu Saravanan  
Bioengineering  
Junior

LAB NAME  
**Tawil Lab**

FACULTY ADVISOR  
**Bill Tawil**

GRADUATE STUDENT DAILY LAB SUPERVISOR  
**N/A**

DEPARTMENT  
**Bioengineering**

## Effect of Platelet Derived Growth Factor (PDGF) Short Peptide on Human Foreskin Fibroblast (HFF) Proliferation and Migration

Chronic wounds are an increasingly prevalent problem in the healthcare industry with the recent rise in diabetes, heart disease, obesity, and other conditions that adversely affect the rate of wound healing. Platelet derived growth factor (PDGF) is an excellent candidate for use in chronic wound therapy due to its potential to increase cellular migration and proliferation. As entire growth factors can be costly and limited in their effective dosages, this paper explores the use of a shorter PDGF-mimetic peptide sequence. In this study, the effects of this PDGF peptide on human foreskin fibroblasts (HFFs) were investigated in vitro using a cell monolayer as well as a previously developed fibrin bead model. HFF proliferation was tested using both a 2D monolayer as well as a 3D fibrin bead model in comparison with a connexin mimetic peptide serving as a positive control and a scrambled sequence as a negative control. HFF migration from a polymerized 3D fibrin bead was studied in comparison to both control peptides as well. It was observed that while the shorter peptide had little proliferative effect, it did significantly increase the migration distances of HFFs out of a fibrin bead over 7 days. It is possible that in vivo, this peptide would be more effective in inducing cellular proliferation and migration. While more studies need to be performed to confirm its effectiveness in comparison with the whole growth factor, these studies suggest the PDGF-mimetic peptide as a promising replacement in chronic wound care.

## Effect of Platelet Derived Growth Factor (PDGF) Short Peptide on Human Foreskin Fibroblast (HFF) Proliferation and Migration in a Novel 3D Fibrin Bead

Veronica S. Hughey<sup>1</sup>, Manu Saravanan<sup>1</sup>, Chase S. Linsley<sup>1</sup>, Benjamin Wu<sup>1,2</sup>, Bill Tawil<sup>1</sup>

<sup>1</sup>. Department of Bioengineering, UCLA, USA

<sup>2</sup>. Division of Advanced Prosthodontics and the Weintraub Center for Reconstructive Biotechnology, UCLA, USA

UCLA Samueli  
School of Engineering  
UNDERGRADUATE RESEARCH PROGRAM

**Abstract**

Platelet derived growth factor (PDGF) is an excellent candidate for use in chronic wound therapy due to its potential to increase cellular migration and proliferation. As entire growth factors can be costly and limited in their effective dosages, this paper explores the use of a shorter PDGF-mimetic peptide sequence. In this study, the effects of this PDGF peptide on human foreskin fibroblasts (HFFs) were investigated in vitro using a cell monolayer as well as a previously developed fibrin bead model. HFF proliferation was tested using both a 2D monolayer as well as a 3D fibrin bead model in comparison with a connexin mimetic peptide serving as a positive control and a scrambled sequence as a negative control. HFF migration from a polymerized 3D fibrin bead was studied in comparison to both control peptides as well. It was observed that while the shorter peptide had little proliferative effect, it did significantly increase the migration distances of HFFs out of a fibrin bead over 7 days. It is possible that in vivo, this peptide would be more effective in inducing cellular proliferation and migration. While more studies need to be performed to confirm its effectiveness in comparison with the whole growth factor, these studies suggest the PDGF-mimetic peptide as a promising replacement in chronic wound care.

**Introduction**

Chronic wounds are a major issue in the healthcare industry, costing the United States between \$20 and \$25 billion dollars a year and affecting up to 8 million patients. Potential therapies are becoming a more vital area of research as conditions such as diabetes, heart disease, and obesity increase the prevalence of complications with wound healing. Although the exact causes of chronic wounds are still under investigation, a study by Vazquez et al. suggested that the problem may stem from a lack of fibroblast proliferation; they observed that the fibroblasts present in chronic wounds had irregular morphologies and proliferated at a much slower rate than those present in curable wounds. PDGF is an especially vital factor, known to increase the proliferation, migration, and extracellular matrix (ECM) deposition of cells in all stages of the wound healing process by acting as a chemoattractant for fibroblasts, smooth muscle cells, and endothelial cells. Currently, the only FDA-approved, commercially available medication involving PDGF for chronic wound therapy is Becaplermin (Regranex®) which consists of a recombinant PDGF BB chain loaded into a carboxymethylcellulose-based gel. One potential resolution would be to use a shorter peptide sequence, one that captures the most effective part of the growth factor but in a shorter format that is easier and more cost-effective to synthesize. The effect of this comparable peptide on HFF migration and proliferation was investigated in vitro using both a 2D and a novel 3D fibrin bead model.

**Materials & Methods**

Human foreskin fibroblasts (HFF) were cultured up to passage 11 and the standard growth media was Dulbecco's Modified Eagle Media (DMEM), 10% fetal bovine serum, 1% antibiotic/antimycotic. Solutions containing either custom peptide or PDGF-BB were made in Serum-Deficient (SD) media (DMEM, 0% fetal bovine serum, 1% antibiotic/antimycotic). All peptides were stored in lyophilized powder form and were reconstituted in Dulbecco's Phosphate-Buffered Saline (DPBS) at a final concentration of 10 µg/mL. The experimental PDGF peptide, designated Peptide A, was of customized sequence Arg-Glu-Cys-Lys. The positive control was the Gap27 peptide designated as Peptide S, was of customized sequence SPTPTKTRP. Finally, the scrambled sequence of the Gap27 peptide which acted as a negative control, Peptide T, was of customized sequence TPEPSSGTRK with the same molecular weight.

**Figure 1:** Experimental design of cell growth in investigation peptide experiments. HFFs were first investigation peptide experiments. Each 2D fibrin bead and allowed to hydrate in standard media for 48 hours and seeded with 25,000 cells and randomized hours before replacement with 3D media supplemented with investigation peptide candidates A, S, and T. An peptide candidates A, S, and T were captured after 48 hours, which produces a fluorescent signal and migration was analyzed via ImageJ on days 1, 3, upon media that can be used by a plate reader, was used, 5, and 7.

**Figure 2:** Experimental design of cell migration in investigation peptide experiments. HFFs were first investigation peptide experiments. Each 2D fibrin bead and allowed to hydrate in standard media for 48 hours and seeded with 25,000 cells and randomized hours before replacement with 3D media supplemented with investigation peptide candidates A, S, and T. An peptide candidates A, S, and T were captured after 48 hours, which produces a fluorescent signal and migration was analyzed via ImageJ on days 1, 3, upon media that can be used by a plate reader, was used, 5, and 7.

**Migration Rates of HFF**

Fig. 3 HFF cell migration measured by ImageJ. Cells were suspended in fibrinogen gel and seeded with fibronectin to form fibrin bead, grew for 7 days in presence of each peptide and media. (A) Summary of HFF cell migration from fibrin beads over 7 days for each experimental condition. Peptide A significantly increased migration in comparison to pure media. (B) Summary of HFF migration seeded from fibrin beads in 3D fibrin wound healing models over 7 days for each experimental condition.

**Proliferative Effect on HFF**

Different concentrations of Peptide A were investigated for their effect on HFF proliferation using both 2D and 3D models. It can be seen that the environment of HFFs may affect their response to different peptides. In figures 5B and 5C, it can be seen that in the 2D model, most of the concentrations control peptides caused an increase in the proliferation of HFFs over 7 days while in the 3D model, there was no significant increase in proliferation in conditions under the influence of the control peptides. For both the 2D and 3D models, there is no significant difference between the control group without peptide and the experimental conditions as can be seen in figures 5A and 5A'. From these trends, it can be concluded that HFFs react differently to factors such as peptide concentrations depending on their mechanical environment, but that not all peptides are affected by this variable in the same way.

**Future Directions**

It is possible that in vivo, this peptide would be more effective in inducing cellular proliferation and migration in conjunction with other key factors in the wound healing process. While more studies need to be performed to confirm its effectiveness in comparison with the whole growth factor using more complex wound healing models, these studies suggest some promise for the replication of the important wound healing functions of PDGF.

**Imaging**

Fig. 6 (A) HFF cells in fibrin beads imaged on days 1, 5, and 7 in pure media. (B) HFF cells in fibrin beads imaged on days 1, 5, and 7 immersed in media spiked with positive control Peptide S. (C) HFF cells in fibrin beads imaged on days 1, 5, and 7 immersed in media spiked with positive control Peptide S.

**Conclusions**

- In this study, a shorter peptide sequence representing a region of PDGF binding interface, Peptide A, was identified and studied for its potential to induce cellular migration or proliferation during wound healing to replace more expensive, potentially harmful therapies like Regranex.
- This study also observed a difference in HFF proliferation between the novel 3D fibrin bead model and the 2D wound healing model. Overall, less proliferation was observed than HFFs seeded the 2D surface, which is less limited by nutrient and waste diffusion. Peptide A did not have a significant effect on the proliferative effect of HFF cells.
- While Peptide A had little effect on HFF proliferation, it did significantly increase the migration distances of HFFs out of a fibrin bead over 7 days. It is logical that having an effect on migration may cause a lessened effect on cellular proliferation; cellular energy being spent on migration may leave less for cellular division.

**References**

- Nunan, Robert, Keith G. Harding, and Paul Martin. "Clinical Challenges of Chronic Wounds: Searching for an Optimal Animal Model to Recapitulate Their Complexity." *Disease Models & Mechanisms* 7.11 (2014): 1205-1213. PMC. Web. 23 May 2017.
- Vazquez, R. "Proliferative Capacity of Venous Ulcer Wound Fibroblasts in the Presence of Platelet-Derived Growth Factor." *Vascular and Endovascular Surgery* 35.4 (2004): 355-60.
- Chen, Zhen, Jessica Yang, Benjamin Wu, and Bill Tawil. "A Novel Three-Dimensional Wound Healing Model." *Journal of Developmental Biology* 3.4 (2014): 198-209. Web. 8 June 2017.
- Robbins, G. et al. Platelet derived growth factor (PDGF) responsive systems formed from human keratinocytes transduced with the PDGF beta receptor gene. *J. Invest. Dermatol.* 120, 742-749 (2005).
- Iyer, K. et al. Keratinocyte Migration in a Three Dimensional In Vitro Wound Healing Model Cultured with Fibroblasts. *Tissue Engineering and Regenerative Medicine* 15, 721-730 (2018).
- Taronegger, R., Jiang, G., Langawe, H. & Håkansson, L. Expression and function of connexin 43 in human granule wound healing and fibroblasts. *PLoS One* 10, e0115234 (2015).
- Das, S., Cole, M. & Tawil, B. Behavior of Human Dermal Fibroblasts in Three-Dimensional Fibrin Gels: Dependence on Fibronectin and Thrombin Concentration. *Tissue Engineering* 10, 942-954 (2004).



Alexander Soohoo  
Chemical Engineering  
Junior

LAB NAME  
**Tang Lab**

FACULTY ADVISOR  
**Yi Tang**

GRADUATE STUDENT DAILY LAB SUPERVISOR  
**Yiu-Sun Hung**

DEPARTMENT  
**Chemical Engineering**

## Engineering of *Penicillium expansum* as a New Heterologous Host for Natural Product Biosynthesis Elucidation

Heterologous expression is a technique commonly used in recombinant DNA technology to elucidate biosynthetic pathways of natural products. Compounds of interest can be investigated by expressing an organism's genomic DNA in a well-studied host. Genetic manipulation is more flexible in heterologous hosts, allowing for efficient discovery of the genes responsible for a compound's production. However, heterologous expression often fails due to differences in intron splicing and protein folding resulting from the large genetic differences between the native organism and the heterologous host. From prior experiments, results from the native organism *Penicillium brefeldianum* in the commonly used host *S. cerevisiae* have been inconsistent. Therefore, the focus turned to developing a new heterologous host, *Penicillium expansum*, to facilitate heterologous expression in *Penicillium* species, as there is likely conservation in chaperone proteins and intron splicing mechanisms of species within a genus. First, CRISPR/Cas9 gene editing and 5-FOA selection were used to generate an auxotrophic strain. Then, diverse groups of previously characterized fungal pathways were expressed to compare the performance of *P. expansum* with established hosts such as *A. nidulans*. The generated *P. expansum* strain will be available as a host for future heterologous expression experiments using *Penicillium* species, allowing for investigation of uncharacterized gene clusters.

**Samueli**  
School of Engineering

UNDERGRADUATE  
RESEARCH PROGRAM

### Engineering of *Penicillium expansum* Heterologous Expression System for Fungal Genome Mining

ALEXANDER M. SOOHOO, Aliyan Abad, Yiu-Sun Hung, Yi Tang  
Department of Chemical and Biomolecular Engineering, University of California, Los Angeles, Los Angeles, CA 90095

#### Introduction

- Fungal natural products have diverse structures and bioactivities.
- Penicillium* has immense potential for the discovery of new natural products,<sup>1</sup> and solving their biosynthesis can lead to understanding of new enzyme mechanisms and new medicines.
- Scientists solve biosynthesis of fungal natural products using heterologous expression,<sup>2</sup> a technique where foreign genes are inserted and expressed in a heterologous host.
- Heterologous expression in filamentous fungi has unique advantages compared to expression in yeast.

**Table 1:** Heterologous expression in filamentous fungi has advantages over the use of species such as *S. cerevisiae*.

	Yeast ( <i>Saccharomyces cerevisiae</i> )	Filamentous Fungi
<b>Advantages</b>	<ul style="list-style-type: none"> <li>Well-established genetic tools</li> <li>Less likely to interfere with exogenous fungal pathways</li> <li>Generally regarded as safe</li> </ul>	<ul style="list-style-type: none"> <li>Can splice fungal introns (only gDNA is needed)</li> <li>With accessory proteins for fungal natural product production</li> </ul>
<b>Disadvantages</b>	<ul style="list-style-type: none"> <li>Cannot splice fungal introns</li> <li>Need genes encoded for the accessory proteins to be expressed</li> </ul>	<ul style="list-style-type: none"> <li>Relatively crowded metabolic background</li> <li>May produce toxic compounds such as mycotoxins</li> </ul>

However, heterologous expression may result with inaccurate splicing patterns.<sup>3</sup> Such mis-splicing issues from heterologous hosts could be due to differences in splicing recognition across different fungal genera.

**Figure 1:** Mis-splicing of *P. expansum*'s PKS-NRPS homolog of mycol in *A. nidulans* would lead to premature stop codons, resulting with non-functional truncated products.

With the abundance of un-solved *Penicillium* gene clusters, development of a heterologous expression system in *Penicillium* can potentially uncover new natural products.

#### Results

- P. expansum* will be evaluated by comparing its production profile with commonly used hosts, such as *A. nidulans*.
- A PKS (polyketide synthase) product from the wortmanninone pathway was used as a probe due to its distinctive yellow color.

**Figure 3:** *P. expansum*'s heterologous expression profile for the selected probe.

- P. expansum*'s heterologous expression is high and stable.

**Figure 4:** PKS product isolation and characterization is more achievable with *P. expansum* heterologous expression.

- PKS product isolation and characterization is more achievable with *P. expansum* heterologous expression due to less shunt or other metabolic production.

**Figure 7:** *P. expansum* has a very clean metabolic background, making it easier to identify target compounds, compared to expression in other hosts.

- Cleaner metabolic background for *P. expansum* could facilitate the identification of the target compounds.

#### Discussion

- In preliminary tests, *P. expansum* has proven to be easy to grow and use for heterologous expression experiments.
- P. expansum* has a strong and clean production profile.
- P. expansum* will be evaluated as a heterologous host by comparing its production profile with the production profiles of other fully elucidated biosynthetic pathways in other commonly used hosts, such as *A. nidulans*.

**Figure 8:** Promoter optimization was performed for *P. chrysogenum*<sup>4</sup> and a similar strategy can be used for *P. expansum*.

- Different promoters were tested for *P. chrysogenum*, which can potentially be used for *P. expansum* as they are of the same genus.
- Overexpression of gene-cluster specific/global transcription factors can elicit the metabolic potential of *P. expansum*.
- Use of *P. expansum* can lead to examination of the intron splicing pattern for genes that are silent in expression in the producing host and be compared with computational predictions.

**Figure 9:** Previous heterologous expression attempts to solve the biosynthetic pathway of these two molecules have been inconclusive, but will be redone with the generation of the *P. expansum* heterologous host strain.

- This new host can be used to revisit biosynthetic pathways (especially in *Penicillium*) that were futile in previous heterologous expression attempts, such as for Brefeldin A and Chaetoglobosin A.
- This general methodology can be applied to more species to allow for generation of more heterologous host organisms in other genera.

#### Designing the Heterologous Expression System

- Current fungal hosts such as *A. nidulans* utilize a plasmid-based heterologous expression system.
- Penicillium expansum* is a suitable candidate as a new heterologous host due to easy genome editing.
- P. expansum* is highly rich in secondary-metabolism gene clusters (25 polyketide synthases (PKSs) and 17 nonribosomal peptide synthetases (NRPSs)).
- The *gpdA* constitutive promoter was chosen for high and stable heterologous expression.

**Figure 2:** In the designed plasmid expression system, it was important to establish a common expression system between *P. expansum* and other commonly used heterologous hosts.

#### Methods

##### Auxotroph Generation

- In a plasmid-based heterologous expression system, the host organism needs to be an auxotroph, which are deficient in genes for essential supplements.
- When a plasmid is transformed with a heterologous host, cells only survive if they have a gene for the supplement production and thus the genes of interest.

**Figure 3:** The *pyrG* gene was knocked out using homology-directed recombination, and replaced with a marker of different size to confirm knockout. The *pyrG* gene was knocked out and replaced with a marker. Only the cells with successful *pyrG* knockout would survive in the presence of 5-FOA.

- Selecting surviving colonies in both cases would allow for generation of a uracil and riboflavin auxotroph.

**Figure 4:** CRISPR/Cas9 was used to generate a *P. expansum* strain without the gene necessary to produce riboflavin on its own.

- CRISPR/Cas9 was used to generate a pyridoxine and riboflavin auxotroph.

#### Conclusions

- Heterologous expression is a valuable tool used to elucidate biosynthetic pathways in well-studied and cultivated model host organisms, such as *A. nidulans*.
- Penicillium* species are part of a promising genus that has struggled in heterologous expression experiments.
- A *Penicillium expansum* strain has been generated, and has shown promising production and metabolic profiles.
- Penicillium expansum*'s performance as a heterologous host will further be evaluated against previously characterized pathways in commonly used hosts.
- Penicillium expansum* can be a complementary or alternative option to existing hosts such as *A. nidulans* to facilitate discovery of natural products.

#### Acknowledgements

- This lab was supported by the UCLA Center for Catalysis and Reaction Engineering.
- This lab was supported by the UCLA Center for Catalysis and Reaction Engineering.
- This lab was supported by the UCLA Center for Catalysis and Reaction Engineering.
- This lab was supported by the UCLA Center for Catalysis and Reaction Engineering.

#### References

- Wang, J.-C., Gonzalez, G., Pagan, S., et al. Science 2010, 328, 1078-1081.
- Wang, J.-C., Gonzalez, G., Pagan, S., et al. Science 2010, 328, 1078-1081.
- Wang, J.-C., Gonzalez, G., Pagan, S., et al. Science 2010, 328, 1078-1081.
- Wang, J.-C., Gonzalez, G., Pagan, S., et al. Science 2010, 328, 1078-1081.



Alison Tran  
Bioengineering  
Junior

LAB NAME

**Meyer Lab**

FACULTY ADVISOR

**Aaron Meyer**

GRADUATE STUDENT DAILY LAB SUPERVISOR

**Moriah Garcia**

DEPARTMENT

**Bioengineering**

## Fluorescently Tagging the Endogenous AXL Gene in MDA-MB-231 Breast Cancer Cells Using CRISPR Intron Knock-In

Many cancer cells undergo epithelial-mesenchymal transition, which leads to metastasis and chemoresistance. Studies have shown that the expression of AXL, a member of the TAM family of receptor tyrosine kinases, contributes to inducing the mesenchymal state. Tagging the endogenous AXL gene with fluorescence would make it easier to study AXL in future research. Traditionally, endogenous genes are tagged by using CRISPR to attach the fluorescence template to the exon at the end of the gene sequence. Instead, by inserting the YFP template into an intron in the AXL gene sequence, the template can be generic. This simplifies the process by reducing the risk of frameshift mutation and allowing for homology-independent repair. Five different intron locations in the AXL gene sequence were chosen and CRISPR was performed to target those specific locations. The cells were then expanded and analyzed by flow cytometry. So far, flow cytometry results have not shown fluorescently tagged cells, but the project is still ongoing. Future experiments include testing whether the flow cytometer can detect the fluorescent tag, using fluorescent gRNA to see if the CRISPR complex is internalized into the cells, and eventually growing the cells out until they can be run through FACS. Successful fluorescent tagging of endogenous AXL would make it easier to visualize and quantify AXL expression in cells in future projects, and understanding AXL is important to improving cancer treatment and chemotherapy.

## Fluorescently tagging AXL in breast cancer cells using intron-based CRISPR

Alison Tran<sup>1</sup>, Linnet Chang<sup>1</sup>, Moriah Garcia<sup>1</sup>, Scott Taylor<sup>1</sup>, Aaron Meyer<sup>1</sup>

<sup>1</sup>Department of Bioengineering, University of California, Los Angeles



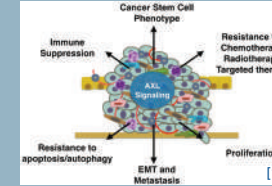
UNDERGRADUATE RESEARCH PROGRAM

### INTRODUCTION

Motivation

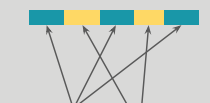
AXL is a receptor in many cancer cells. It is known for driving epithelial-mesenchymal transition (EMT), making the cells more resistant to apoptosis and chemotherapy.

Goal  
If we were able to fluorescently tag the endogenous AXL gene in cancer cells, it would make AXL expression easier to study in future projects.



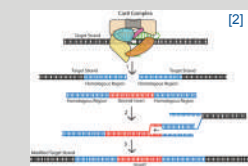
### INTRON-BASED CRISPR

DNA Sequence



**Exons:** Used to code for protein, editing could cause mutation in protein  
**Introns:** Does not contain code for protein, so cannot mutate protein

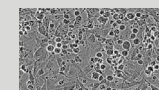
CRISPR to insert fluorescence DNA



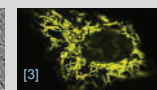
Inserting the DNA template into an intron (instead of the traditional method of inserting into an exon) reduces the risk of frameshift mutation

### METHOD

Materials



**MDA-MB-231 Breast Cancer Cells:** These cells express high, varying levels of AXL, so they will fluoresce if the CRISPR is successful.



**Yellow Fluorescent Protein (YFP) vs DNA template:** The AXL gene will be tagged with YFP, which fluoresces yellow.



**CRISPR Reagents:**  
-- Cas9: cuts DNA  
-- gRNA: guides the Cas9 to the intron to cut at

Procedure

1. Use CRISPR reagents to deliver the YFP template to the breast cancer cells.

	Experimental	Control #1	Control #2
Condition	Contains everything needed for successful CRISPR	Used to determine if Cas9 or YFP template have any other effect on cells	Cells only growing in normal media
Reason	If successful, endogenous AXL gene will be fluorescently tagged!	Contains everything except gRNA (used to target intron)	Used to see how normal MDA-MB-231 cells grow

2. Run cells through flow cytometry to determine whether cells are fluorescent.  
-- Flow cytometry measures the fluorescence of cells and graphs the population of cells.

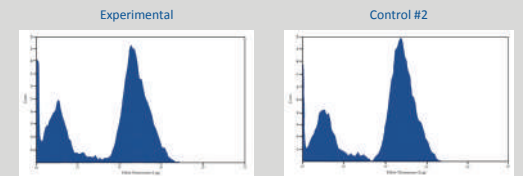
### RESULTS

Cell Growth



The experimental cells are at the same confluency as the control #2 cells, while the control #1 cells are at a lower confluency.  
• However, because the CRISPR (experimental) cells and the control #2 (cells only) cells grew at the same rate, this is not a problem.

Flow Cytometry



Flow cytometry results showed no difference in yellow fluorescence between the CRISPR (experimental) cells and the control #2 (cells only) cells.  
• This means that the CRISPR was not successful in fluorescently tagging AXL.

### ONGOING EXPERIMENTS

Because the CRISPR was unsuccessful, we will perform new preliminary experiments to determine what went wrong:

- Testing whether the flow cytometer can detect yellow fluorescence
- Using a fluorescent gRNA to see if the CRISPR complex is internalized into the cells

Once we are able to successfully use CRISPR to fluorescently tag AXL, the cell population will be run through fluorescence activated cell sorting (FACS) to obtain a pure population of only cells with fluorescently tagged AXL.

### CONCLUSION

- While thus far, we have been unable to successfully fluorescently tag the endogenous AXL gene in MDA-MB-231 breast cancer cells, this project is still ongoing.
- We have figured out the exact procedures for performing CRISPR, which will make it easier to optimize once the CRISPR is successful.
- This project will continue until we are able to fluorescently tag AXL.

### ACKNOWLEDGMENTS

We would like to thank the UCLA Bioengineering Department, the UCLA Engineering URP, the Roy Wollman lab, and NIH DP5-00019815.



### REFERENCES

- [1] <https://www.mdpi.com/2073-6694/8/11/103>
- [2] <http://www.plantphysiol.org/content/135/1/25.full>
- [3] <https://www.biocat.com/proteomics/yellow-fluorescent-proteins-yfp-s>
- [4] <https://www.sciencenews.org/article/crispr-spinoff-gene-editor-causes-unintended-typos-dna>



Peter Wang  
Chemical Engineering  
Junior

LAB NAME

N.1 Labs

FACULTY ADVISOR

Dean Ho & Chih-Ming Ho

GRADUATE STUDENT DAILY LAB SUPERVISOR

Theodore Kee

DEPARTMENT

Bioengineering

## Prospective Modulation of Combination Chemotherapy Dosing in a Metastatic Castration-Resistant Prostate Cancer Patient using CURATE.AI, an Artificial Intelligence Platform

Conventional chemotherapy typically determines an appropriate drug regimen using dose escalation to reach a maximum tolerated dose or via dose expansion, often resulting in high toxicity experienced by the patient. In combination therapy for oncology, finding the appropriate and optimal dose combination is further exacerbated, as drug synergy is dose- and time- dependent with patient variability. To address dynamic drug synergy and dose optimization, we developed CURATE.AI, an artificial intelligence platform, using a powerful correlation termed phenotypic response surface, which has been clinically validated and has optimized patient liver transplant immunosuppression, and tuberculosis and HIV therapy. In this case report, we outline the CURATE.AI guided treatment of an 82-year-old male patient participating in a Phase 1B/2A safety and tolerability study of a novel inhibitor, in combination with enzalutamide, to address metastatic castration-resistant prostate cancer (mCRPC) by reducing serum prostate-specific antigen (PSA) levels. CURATE.AI identified a dose combination that was 50% lower than the patient's originally assigned dose regimen prior to CURATE.AI-guided dosing, and successfully identified substantial dose adjustments, increasing both treatment efficacy and tolerance. The reduction in PSA levels during CURATE.AI guided treatment was validated by computed tomography (CT) imaging and nuclear medicine bone scan, which showed a sustained decrease in tumor lesion size, demonstrating no further disease progression.



## Prospective Modulation of Combination Chemotherapy Dosing in a Metastatic Castration-resistant Prostate Cancer Patient using CURATE.AI, an Artificial Intelligence Platform



Peter Wang<sup>1,2</sup>, Theodore Kee<sup>2,3</sup>, Jeffrey Khong<sup>4</sup>, Allan J. Pantuck<sup>5</sup>, Arie S. Beldegrun<sup>6</sup>, Chih-Ming Ho<sup>6</sup>, and Dean Ho<sup>2,3,7,8</sup>

<sup>1</sup>Department of Chemical and Biomolecular Engineering, University of California, Los Angeles, Henry Samueli School of Engineering and Applied Science, <sup>2</sup>Singapore Institute for Neurotechnology (SINAPSE), National University of Singapore, <sup>3</sup>Department of Biomedical Engineering, NUS Engineering, National University of Singapore, <sup>4</sup>Department of Computational and Systems Biology, University of California, Los Angeles, <sup>5</sup>Ronald Reagan UCLA Medical Center, Department of Urology, David Geffen School of Medicine, Institute of Urologic Oncology, University of California, Los Angeles, <sup>6</sup>Department of Mechanical and Aerospace Engineering, University of California, Los Angeles, Henry Samueli School of Engineering and Applied Science, <sup>7</sup>Department of Pharmacology, Yong Loo Lin School of Medicine, National University of Singapore, <sup>8</sup>Biomedical Institute for Global Health Research and Technology (BIGHEART), National University of Singapore.

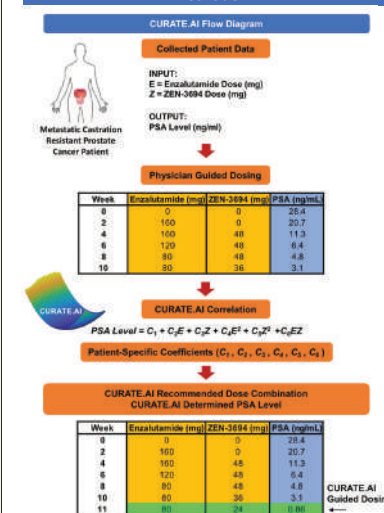
Overview

Conventional chemotherapy typically determines an appropriate drug regimen using dose escalation to reach a maximum tolerated dose (MTD) or via dose expansion, often resulting in high toxicity experienced by the patient. In combination therapy for oncology, finding the appropriate and optimal dose combination is further exacerbated, as drug synergy is dose- and time-dependent with intra- and inter-patient variability. To address dynamic drug synergy and dose optimization, we developed CURATE.AI, an artificial intelligence (AI) platform, using a powerful correlation termed phenotypic response surface (PRS), which has been clinically validated and has optimized patient liver transplant immunosuppression, and tuberculosis and HIV therapy.

Introduction

In this case report, we outline the CURATE.AI guided treatment of an 82-year-old male patient participating in a Phase 1B/2A safety and tolerability study of ZEN-3694, a novel inhibitor, in combination with enzalutamide, an androgen receptor inhibitor, to address metastatic castration-resistant prostate cancer (mCRPC) by reducing serum prostate-specific antigen (PSA) levels. CURATE.AI identified a dose combination that was 50% lower than the patient's originally assigned dose regimen prior to CURATE.AI-guided dosing, and successfully identified substantial dose adjustments, increasing both treatment efficacy and tolerance. The reduction in PSA levels during CURATE.AI guided treatment was validated by computed tomography (CT) imaging and nuclear medicine bone scan, which showed a sustained decrease in tumor lesion size, demonstrating no further disease progression.

Methods



**Clinical Protocol:**

- Patient was enzalutamide-naïve and was recruited at the University of California, Los Angeles site.
- He provided written informed consent to participate in a nonrandomized, open label, phase 1b/2a clinical trial (ClinicalTrials.gov Number: NCT02711956; UCLA IRB #16-000320) of ZEN-3694 in combination with enzalutamide.
- Clinical activity was assessed by PSA and radiographic response by CT imaging and nuclear medicine bone scans as defined by PCWG2 criteria

**CURATE.AI-Guided Dosing:**

- The clinical team obtained and recorded the patient's PSA levels, drug regimen dosages, and other clinical events such as infection.
- Collected data were used to construct the CURATE.AI profiles, which visually represented a calibration of the patient's phenotypic response surface correlating the PSA levels (ng mL<sup>-1</sup>) to the drugs' dosage values (mg).

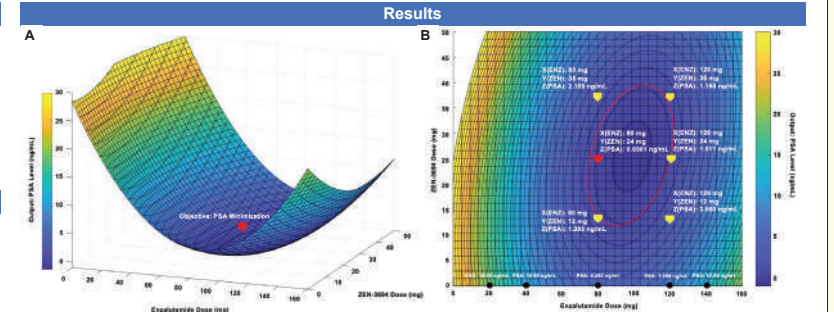


Figure 1. CURATE.AI calibration of patient's CURATE.AI profile with enzalutamide and ZEN-3694 doses and PSA levels. A) The patient's CURATE.AI profile is shown. Using the patient's profile, the objective of minimizing the patient's PSA level is achievable by recommending the appropriate dose adjustments of enzalutamide and ZEN-3694 (red arrow). B) CURATE.AI profile recommended combination of 24 mg ZEN-3694 and 80 mg enzalutamide (red arrow).

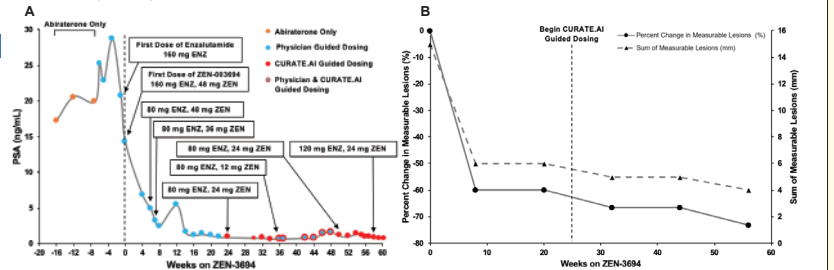


Figure 2. Summary of patient's radiographic assessments and the patient's recorded PSA levels. A) The patient's percent change in measurable lesion, an aortocaval lymph node, from baseline (solid) and sum of measurable lesion(s) (dashed) during treatment period are shown. B) The patient's recorded PSA levels during treatment period are shown. PSA levels are labeled with physician-guided dosing (blue) or CURATE.AI-guided dosing (red) adjustments to the patient's enzalutamide or ZEN-3694 dose.

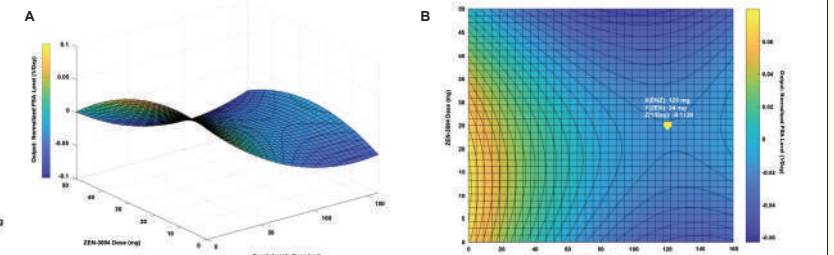


Figure 3. CURATE.AI PSA slope analysis. A) The patient's CURATE.AI normalized PSA level slope analysis is shown. B) The CURATE.AI recommended combinations of 24 mg ZEN-3694 and 120 mg enzalutamide (yellow) is shown.

Conclusion

In this study, CURATE.AI identified a dose combination that was 50% lower than the patient's originally assigned dose regimen prior to CURATE.AI-guided dosing, and CURATE.AI-guided dosing resulted in no further disease progression. As demonstrated in this case report, CURATE.AI can be broadly applied to liver transplant, oncologic indications, and many other disease indications. In the context of digital medicine, CURATE.AI represents the advancement and utilization of AI to overcome challenges encountered in the clinic and conventional approaches to medicine such as MTD for combinatorial therapy.

Acknowledgement

We gratefully acknowledge the UCLA Institute of Urologic Oncology team members, as well as the patient and family members. D.H. gratefully acknowledges support from the V Foundation for Cancer Research and Wallace H. Coulter Foundation.

References

1. Zarrinpar A, et al. (2016) Individualizing liver transplant immunosuppression using a phenotypic personalized medicine platform. *Sci. Transl. Med.* 8(333):333ra349.
2. Pantuck AJ, et al. (2018) Modulating BET bromodomain inhibitor ZEN-3694 and enzalutamide combination dosing in a metastatic prostate cancer patient using CURATE.AI, an artificial intelligence platform. *Advanced Therapeutics* 1(6):1600104.





William Whitehead  
Electrical Engineering  
Junior

LAB NAME  
**Connection Lab**

FACULTY ADVISOR  
**Jeff Burke**

GRADUATE STUDENT DAILY LAB SUPERVISOR  
**N/A**

DEPARTMENT  
**Theater, Film, and Television**

## Scene Segmentation with Warped Crops to Enhance the Foveal Region

Scene segmentation is the task of breaking up a picture into segments, where each segment indicates a different type of object, such as a wall or chair. Deep neural networks are the best current technology to perform this task; here we consider a convolutional neural network (CNN) that is trained to identify what type of object exists at the center of an image crop. The crop comes from a sliding window, or field of view, that is applied to the scene being segmented. At the boundary between two regions in an image, translating the field of view by one pixel should result in a different classification. Even for people, this is hard; two images that are shifted by one pixel look pretty much the same. With the goal of making segmentation more accurate, we introduce the idea of warped crops to make the difference between adjacent field of views more obvious. The crops are warped so that the center of the field of view (the foveal region) is magnified relative to the periphery, such that small translational changes to the field of view create a greater change in the appearance of the crop while keeping information at the periphery, which is not magnified. Motivation for this sort of warping also comes from cortical magnification, the phenomena of human retinas having a higher density of photoreceptors in the fovea than at the periphery. We find that these warped crops do yield a small improvement in segmentation.

# Scene Segmentation with Warped Crops to Enhance the Foveal Region

UCLA Samueli School of Engineering  
William Whitehead, Jeff Burke

**Abstract**

Scene segmentation is the task of breaking up a picture into segments, where each segment indicates a different type of object, such as a wall or chair. Deep neural networks are the best current technology to perform this task; here we consider a convolutional neural network (CNN) that is trained to identify what type of object exists at the center of an image crop. The crop comes from a sliding window, or field of view, that is applied to the scene being segmented. At the boundary between two regions in an image, translating the field of view by one pixel should result in a different classification. Even for people, this is hard; two images that are shifted by one pixel look pretty much the same. With the goal of making segmentation more accurate, we introduce the idea of warped crops to make the difference between adjacent field of views more obvious. The crops are warped so that the center of the field of view (the foveal region) is magnified relative to the periphery, which is not magnified. Motivation for this sort of warping also comes from cortical magnification, the phenomena of human retinas having a higher density of photoreceptors in the fovea than at the periphery. We find that these warped crops do yield a small improvement in segmentation.

**The Task: Semantic Scene Segmentation**

Figure 1. A scene, to be segmented; we want to know where different things, such as cars and pedestrians, are.

Figure 2. The scene, segmented; different colors show where things are in the image. This segmentation was generated by one of our algorithms.

**Existing Methods: Deep Learning for Segmentation**

- Convolutional Neural Networks (CNNs) trained to classify pixels or regions in an image
- Simple Fully-convolutional networks (FCNs) are an efficient implementation
- But advanced FCNs cannot be decomposed into a classifier for individual pixels
- This work thinks in terms of classifying individual pixels or regions

Figure 3. To produce a segmentation, we split a scene into regions using a super-pixel algorithm. The centers of these super-pixels are then taken as the center of crops; the crops, shown in the center, are classified by a Neural Network and the results are assigned back to the super-pixels to form a segmentation.

**Introducing Warped Crops**

- Since a crop is used to classify only the very center of an image, we should magnify the center that we are classifying
- By warping the crop instead of just shrinking the field-of-view (FOV), the center becomes magnified without losing peripheral information
- Analogous to the Cortical Magnification that exists in human vision
- This idea is good under the assumption that CNNs will not actually learn to treat the center of a crop as more important than other parts of the crop

Figure 4. A regular (un-warped) crop is on the left; warping and zooming in on the center, we reach the crop on the right. Warping can be used in varying amounts, described by A and B parameters.

Figure 5. As the window of a warped crop pans across a scene to classify different regions, the appearance of the crop changes dramatically. The frame on the right shows locations in a scene that the warped crops are centered on.

**Describing Warped Crops by Formula**

Figure 6. Warping is described by common functions which show how space changes when crops are warped.

Mapping points in a scene  $S$  to points in a crop  $C$ , in polar coordinates:

$$C[r_c, \theta_c] = S[r_s, \theta_s]$$

Normalizing the relationship between the radius in the scene and the radius in the crop.  $S_s$  is the size of the scene,  $S_c$  is the size of the crop, and  $f_{\omega}$  adjusts the field-of-view.

$$r_s = f_{\omega} \left( \frac{r_c}{S_c} \right) * f_{\omega} * S_s$$

Defining a characteristic function for a particular shape of warping;  $r_s$  is the normalized crop radius,  $f_{\omega}(r_s)$  is the normalized radius in the scene.

$$f_{\omega}(r_s) = A r_s + B r_s^2$$

**Performance Results – Benchmark Scores and Heatmaps**

Figure 7. Results and select heatmaps from the ADE20K dataset; heatmaps created using warped crops are much better at delineating regions.

Results are often quantified by the mean intersection over union (mIoU), which measures the intersection over union (True Positives)/(True Positives + False Positives + False Negatives) for each prediction class and averages them.

Table 1. Results from Cityscapes dataset, comparing our scores (first two) with results from advanced FCN methods.

Network design	mIoU score
MobileNetv2, A=1 B=0	0.53
MobileNet, A=0 B=1	0.68
DeepLab FCN [1]	0.71
DPC-MobileNet FCN [2]	0.75

Table 2. Scores on ADE20K dataset, again first two scores are ours.

Network design	mIoU score
MobileNet, A=1 B=0	0.29
MobileNet, A=0 B=1	0.31
FCN baseline [8]	0.34
EnNet FCN [9]	0.41

**Concluding Thoughts**

- Crop warping performs better than our baseline without warping, especially on the Cityscapes dataset;
- However, we do not match state-of-the-art results, and segmentation by classification of pixels is computationally slow
- Instead, emphasize the ideas that led to crop warping, and try to better understand why crop warping improved results
- Can segmenting pixel by pixel make us realize something that is not apparent in FCN segmentation?

**Acknowledgements**

This research has been made possible by funding from the UCLA Internet Research Initiative (IRI), computation resources from the UCLA CHIPS laboratory, and support from the Samueli Undergraduate Research Program.

**References**

- [1] L. Chen, G. Papandreou, I. Kokkinos, K. Murphy, and A. L. Yuille. Deeplab: Semantic image segmentation with deep convolutional nets, atrous convolution, and fully connected crf. *IEEE Transactions on Pattern Analysis and Machine Intelligence*, 40(4):834–848, April 2018.
- [2] Liang-Chieh Chen, Maxwell Collins, Yukun Zhu, George Papandreou, Barret Zoph, Florian Schroff, Hartwig Adam, and Jon Shlens. Searching for efficient multi-scale architectures for dense image prediction. In *Advances in Neural Information Processing Systems 31*, pages 8099–8710. Curran Associates, Inc., 2018.
- [3] Marcus Cordts, Mohamed Omran, Sebastian Roth, Timo Rothfeld, Markus Ennenkes, Rodrigo Benenson, Uwe Franke, Stefan Roth, and Bernt Schiele. The cityscapes dataset for semantic urban scene understanding. In *Proc. of the IEEE Conference on Computer Vision and Pattern Recognition (CVPR)*, 2016.
- [4] Kaiming He, Wanglun Shao, Shaoqing Ren, and Jian Sun. Identity mappings in deep residual networks. In *Computer Vision – ECCV 2016*, pages 630–645, Cham, 2016. Springer International Publishing.
- [5] J. Long, E. Shelton, and T. Darrell. Fully convolutional networks for semantic segmentation. In 2015 IEEE Conference on Computer Vision and Pattern Recognition (CVPR), pages 3431–3440, June 2015.
- [6] Mark B. Sandler, Andrew G. Howard, Menglong Zhu, Andrey Zhmoginov, and Liang-Chieh Chen. Mobilenetv2: inverted residuals and linear bottlenecks. 2018 IEEE/CVF Conference on Computer Vision and Pattern Recognition, pages 4510–4520, 2018.
- [7] Panqu Wang and Garrison W. Cottrell. Central and peripheral vision for scene recognition: A neurocomputational modeling exploration. *Journal of Vision*, 17(9), June 2017.
- [8] Hong Zhang, Motoki Daira, Junping Shi, Zhongqiang Zhang, Honggang Wang, Anish Tiyyi, and Alexei Avidov. Context encoding for semantic segmentation. In *CVPR*, 2018.
- [9] Boqi Zhou, Hang Zhao, Xavier Puig, Sanja Fidler, Adelia Barrios, and Antonio Torralba. Semantic understanding of scenes through the ade20k dataset. arXiv preprint arXiv:1808.05442, 2018.

If you would like to find out more about the Undergraduate Research Program,  
please contact Director William Herrera:

**William Herrera**

Director

Undergraduate Research Program

310.825.9478

[williamh@seas.ucla.edu](mailto:williamh@seas.ucla.edu)

Engineering Student Resource Center, 6288 Boelter Hall

Or visit our website at <https://tinyurl.com/uclaurp>.

**UCLA** **Samueli**  
School of Engineering

Undergraduate Research Program at the Engineering Student Resource Center  
Office of Academic and Student Affairs  
UCLA Samueli School of Engineering  
420 Westwood Plaza, 6288 Boelter Hall, Los Angeles, CA, 90095-1600  
310.825.9478 | [www.samueli.ucla.edu](http://www.samueli.ucla.edu)